

# Concentration Dependence of the Methane Structure in Silicalite-1: A Molecular Dynamics Study Using the Møller–Plesset-Based Potential

C. Bussai,<sup>†,‡</sup> S. Fritzsche,<sup>‡</sup> R. Haberlandt,<sup>‡</sup> and S. Hannongbua<sup>\*,†</sup>

Department of Chemistry, Faculty of Science, Chulalongkorn University, Bangkok 10330, Thailand, and Department of Molecular Dynamics/Computer Simulations, Institute for Theoretical Physics (ITP), Faculty of Physics and Geoscience, University of Leipzig, Augustusplatz 10-11, 04109, Leipzig, Germany

Received December 20, 2004. In Final Form: January 18, 2005

Møller–Plesset perturbation-based potentials have been used in molecular dynamics simulations to examine methane diffusion in silicalite-1. The simulation box contains 2 unit cells of silicalite-1 and varying loading numbers ( $n_{ld}$ ) from 1, 2, 3, to 4 methane molecules per intersection, corresponding to 8, 16, 24, and 32 molecules per simulation box, respectively. Consistent with the previous study, a preferential diffusing path for methane is close to the channel axes. The structure of the methane molecules in the silicalite-1 pore was exhibited in terms of the methane–methane radial distribution function (RDF) in which the first peak appears at 6.4 Å for  $n_{ld} \leq 2$ , becomes a broad maximum at  $n_{ld} = 3$ , and splits into two sharp peaks centered at 6.4 and 8.6 Å at  $n_{ld} = 4$ . This fact can be clearly described by an intensification of the methane density in the straight and zigzag channels but a decrease in the intersection when the loading increases. These features of the observed RDFs are in contrast with the previous report using a molecular dynamics force-field potential in which the RDFs for all concentrations show first maxima at  $\sim 4$  Å. The analysis of the relative residence times of methane at different sites inside the silicalite suggests that the zigzag channel is the most favored location. The computed self-diffusion coefficients as well as the heat of adsorptions are in reasonable agreement with the available values.

## 1. Introduction

Diffusion and adsorption of molecules in the pores of zeolites are fundamental attributes of many industrial separation and also catalytic processes,<sup>1–4</sup> hence, the importance of the proper representation of diffusion in zeolitic material systems. Despite extensive research, the simple methane diffusion in dealuminated ZMS-5 crystal, namely, silicalite-1, is still not clearly understood yet. On one side, the experimental data for the diffusion coefficient show, for some substances, variations of several orders of magnitude depending on the method used: quasielastic neutron scattering (QENS), pulsed-field gradient nuclear magnetic resonance (PFG–NMR) (microscopic methods), and zero-length column, frequency response, and isotope exchange (macroscopic methods).<sup>5,6</sup> On the other side, although molecular simulation techniques have become an essential tool for studying the diffusivity of guest molecules in zeolites, in particular, molecular dynamics (MD) simulations and the results are in good agreement with those obtained from microscopic (e.g., in NMR

experiments depending, however, on the potential function used.<sup>7–11</sup>

Although several other papers deal with structural properties<sup>2</sup> for the diffusion of methane molecules in silicalite-1, the only available data on the arrangement of methane inside silicalite-1 pores in terms of the radial distribution function, according to our best knowledge, are the molecular dynamics simulations made by us,<sup>11</sup> Demontis et al.<sup>12,13</sup> using a force-field Lennard–Jones potential, and Nicholas et al.<sup>14</sup> using MM2.<sup>15</sup>

Interestingly, the diffusion coefficients at various loadings obtained from various simulations<sup>12,13,14</sup> based on different force-field potential functions are in good agreement with those of the PFG–NMR measurements.<sup>16</sup> This indicates that dynamic properties are not sensitive to the potential function used as well as the assumption employed, etc., i.e., the united atom approximation for a guest molecule, implicit treatment of an Si atom in the silicalite-1 structure,<sup>12,13</sup> although these facts are known to be the sources of discrepancies of the potential hypersurface in terms of both the depth and the shape as well as the

\* To whom correspondence should be addressed. Telephone: 0662-218-7602. Fax: 0662-218-7603. E-mail: supot.h@chula.ac.th.  
<sup>†</sup> Chulalongkorn University.

<sup>‡</sup> University of Leipzig.

(1) Kärger, J.; Ruthven, D. M. *Diffusion in Zeolites and Other Microporous Solids*; Wiley: New York, 1992.

(2) Theodorou, D. N.; Snurr, R. Q.; Bell, A. T. Molecular dynamics and diffusion in microporous materials, in *Comprehensive Supramolecular Chemistry*; Alberti, G., Bein, T., Eds., Pergamon Press: New York, 1996; Vol. 7, p 507.

(3) Keil, F. J.; Krishna, R.; Coppens, M. O. *Rev. Chem. Eng.* **2000**, *16*, 71.

(4) Reyes, S. C.; Sinfelt, J. H.; DelMartin, G. J. *J. Phys. Chem. B* **2000**, *104*, 5750.

(5) Kärger, J.; Ruthven, D. M. *Zeolites* **1989**, *9*, 267.

(6) Ruthven, D. M. *Stud. Surf. Sci. Catal.* **1995**, *97*, 223.

(7) Demontis, P.; Suffritti, G. B. *Chem. Rev.* **1997**, *97*, 2845.

(8) Gergidis, L. N.; Theodorou, D. N.; Jobic, H. *J. Phys. Chem. B* **2000**, *104*, 5541.

(9) Jost, S.; Bär, N. K.; Fritzsche, S.; Haberlandt, R.; Kärger, J. *J. Phys. Chem. B* **1998**, *102*, 6375.

(10) Snurr, R. Q.; Kärger, J. *J. Phys. Chem. B* **1997**, *101*, 6469.

(11) Bussai, C.; Fritzsche, S.; Haberlandt, R.; Hannongbua, S. *J. Phys. Chem. B* **2004**, *108*, 2104.

(12) Demontis, P.; Fois, E. S.; Suffritti, G. B.; Quartieri, S. *J. Phys. Chem.* **1992**, *96*, 1482.

(13) Demontis, P.; Fois, E. S.; Suffritti, G. B.; Quartieri, S. *J. Phys. Chem.* **1990**, *94*, 4329.

(14) Nicholas, J. B.; Trouw, F. R.; Mertz, J. E.; Iton, L. E.; Hopfinger, A. *J. Phys. Chem.* **1993**, *97*, 4149.

(15) Burkert, U.; Allinger, N. L. *Molecular Mechanics*; American Chemical Society: Washington, DC, 1982.

(16) Caro, J.; Bülow, M.; Schirmer, W.; Kärger, J.; Heink, W.; Pfeifer, H. *J. Chem. Soc., Faraday Trans. 1* **1985**, *81*, 2541.

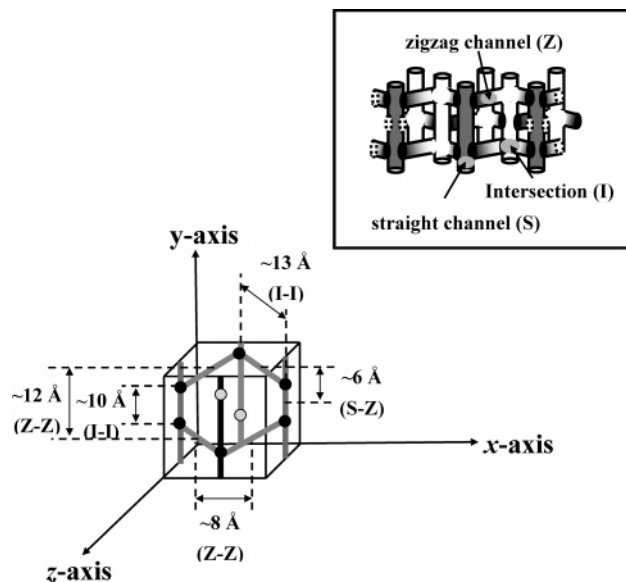


**Figure 1.** Topology of zigzag channel, straight channel, and intersection in the unit cell of silicalite-1 and related distances along the  $x$ ,  $y$ , and  $z$  axes.

position of the potential minima.<sup>11</sup> Such approximations may not reflect the mean dynamical properties that are averaged from trajectories of all channels of silicalite-1 but lead directly to the loss of specific details in structural data in specific channels. Most recently, the use of *ab initio* derived potential in molecular dynamics simulations have shown the power to determine a proper structure of diffusive water molecules in silicalite-1 channels.<sup>17–19</sup>

Here, we perform molecular dynamics simulations using the newly developed *ab initio* fitted potentials<sup>11</sup> and present the results in terms of dynamical and structural information. The simulations are performed at various loadings in a range of 1–4 methane molecules per intersection. The pertinent structural results on methane arrangements are in contrast with the previous studies.<sup>12,14</sup>

## 2. Simulation Details

The crystallographic cell of silicalite-1 ( $\text{Si}_{96}\text{O}_{192}$ )<sup>20</sup> is presented by the  $Pnma$  space group, with lattice parameters  $a = 20.07$  Å,  $b = 19.92$  Å, and  $c = 13.42$  Å. Figure 1 portrays the topology of the zigzag channel (Z), the straight channel (S), and the intersection (I) in the unit cell of silicalite-1 and their distances. The channel structures are shown in an inset of Figure 1, in which the straight and zigzag channels are interconnected at the intersection.

The simulation box is arranged by a  $1 \times 1 \times 2$  unit of silicalite-1, where the loading numbers ( $n_{\text{ld}}$ ) are set to 1, 2, 3, and 4 methane molecules per intersection, corresponding to 8, 16, 24, and 32 methane molecules per simulation box, respectively. The flexibility of the lattice often takes effect as a heating bath that may sterically raise or lower particle diffusion and exchange their energy with those migrating molecules. However, it has been found that the flexibility of the silicalite-1 framework plays an insignificant role on both the dynamical and structural properties of small guest diffusivity.<sup>8–14,17–19</sup> We, thus, kept the lattice fixed through the study. Periodic boundary conditions have been applied. The shifted force potentials have recently proven to be

(17) Bussai, C.; Fritzsche, S.; Hannongbua, S.; Haberlandt, R. *Chem. Phys. Lett.* **2002**, *354*, 310.

(18) Bussai, C.; Vasenkov, S.; Liu, H.; Böhlmann, W.; Fritzsche, S.; Hannongbua, S.; Haberlandt, R.; Kärger, J. *Appl. Catal., A* **2002**, *232*, 59.

(19) Bussai, C.; Fritzsche, S.; Haberlandt, R.; Hannongbua, S. *J. Phys. Chem. B* **2003**, *107*, 12444.

(20) Olson, D. H.; Kokotailo, G. T.; Lawton, S. L.; Meier, W. M. *J. Phys. Chem.* **1981**, *85*, 2238.

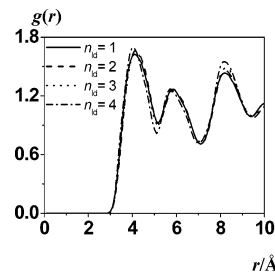


**Figure 2.** Radial distribution functions,  $g(r)$ , from oxygen atoms of silicalite-1 surface to carbon atoms of the methane molecule at various loadings ( $n_{\text{ld}}$ ).

efficient for the evaluation of the Coulombic interaction,<sup>11,17–19,21,22</sup> and is therefore used in this study. The time step of a 1 fs was used to maintain the energy conservation at 300 K. The evaluation part of each run corresponds to a trajectory length of 10 ns after a 1 ps thermalization period.

*Ab initio* fitted potential models based on the second-order Møller–Plesset perturbation (MP2) methods have been used to represent the interactions between methane/methane and silicalite-1/methane. The MP2 fitted methane/methane potential proposed by Rowley et al.<sup>23</sup> was developed from 11 relative orientations of the two methane molecules as a function of C–C separation, where the pairwise parameters were used to represent dispersive and repulsive interactions of C–C, C–H, and H–H. In a similar manner, the *ab initio* silicalite-1/methane interaction energies at the MP2 level were fitted to an analytical form, where the interactions between the C and H atoms of the methane molecule and the Si and O atoms of the silicalite-1 in different channels were treated separately.<sup>11</sup> The optimal methane/methane and silicalite-1/methane interaction energies are  $\sim -0.4$  and  $\sim -5.0$  kcal mol<sup>-1</sup>, respectively.

## 3. Results and Discussions

### 3.1 Radial Distribution Function (RDF).

**3.1.1 Silicalite-1/Methane.** Figure 2 displays RDFs from the oxygen atom on the surface of the silicalite to the C atom of the methane molecule at various loadings. The RDFs are almost concentration-independent, showing the first three maxima around 4.2, 5.8, and 8.3 Å. Methane molecules lying under the first peak are interpreted as those diffusing along the line parallel to the surface at the center of the channels (the diameter of the cylinder-like channel is  $\sim 8.2$  Å). This behavior supports that reported for the diffusion of methane<sup>12</sup> in silicalite-1 at the  $n_{\text{ld}} = 3$  and of water<sup>19</sup> in silicalite-1 at  $n_{\text{ld}} \leq 6$ . Consistent with those proposed in ref 12, the other peaks at 5.8 and 8.3 Å are assigned to methane molecules, where the peak positions correspond to the distances from carbon atoms of methane to oxygen atoms of the nearest 10-oxygen-membered ring and of other adjacent rings on the silicalite-1 surface, respectively. These are similar to those found for water molecules in silicalite-1, only slightly different to the position of the second peak at 6 Å.<sup>19</sup>

**3.1.2 Methane/Methane.** Further information can be attained in regard to the guest–guest radial distribution function as depicted in Figure 3a, with the RDFs between centers of the two methane molecules as a function of loading. For comparison, the RDFs taken from ref 14 are also given (Figure 3b).

The methane–methane RDFs for  $n_{\text{ld}} \leq 2$  display the first apparent maximum at 6.4 Å with the corresponding minimum at 8.2 Å. The transition concentration for methane residence sites starts to be detected at  $n_{\text{ld}} = 3$ ;

(21) Wolf, D.; Keblinski, P.; Phillpot, S. R.; Eggebrecht, J. *J. Chem. Phys.* **1999**, *110*, 8254.

(22) Dufner, H.; Kast, S. M.; Brickmann, J.; Schlenkrich, M. *J. Comput. Chem.* **1997**, *18*, 660.

(23) Rowley, R. L.; Pakken, T. *J. Chem. Phys.* **1999**, *110*, 3368.

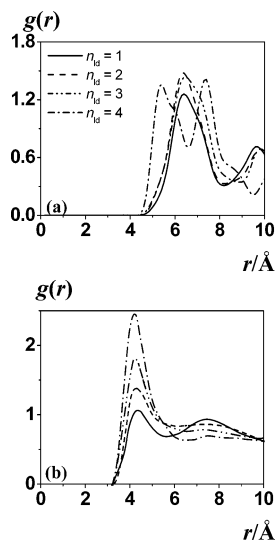


**Figure 3.** Radial distribution functions,  $g(r)$ , between the center of mass of the two methane molecules at various loadings ( $n_{ld}$ ) obtained from this paper (a) and from ref 14 (b).

a first broad maximum at 6.4 Å is established with a minimum at 8.6 Å, which hinted at a substantial transfer of preferential locations of methane molecules from one to another channel. The situation is totally changed at  $n_{ld} = 4$ , where the RDF splits into two sharp peaks. The first distinct peak appears at 5.4 Å, followed by a clear shoulder at 6.2 Å and a minimum at 6.6 Å. The second sharp peak at 7.4 Å is shown with a pronounced shoulder at 8.4 Å.

The current results completely disagree with the previous report using a molecular dynamics force-field potential<sup>14</sup> (Figure 3b), in which the RDF plots for all concentrations show first maxima at  $\sim 4$  Å. There, the authors were not successful in making the first peak disappear for dilute concentrations, e.g.,  $n_{ld} < 1$ , because molecules were not supposed to spend appreciable time in contact.<sup>14</sup> They describe this artifact as the contribution of the methane–methane potential used. However, we have stated, in our previous work,<sup>11</sup> that such artificial features of the structural data can be the result of an unbalance of the guest–guest and guest–framework interactions; i.e., the second pair overestimates the overall interactions. In other words, the methane molecules at such low concentrations are supposed to coordinate to the surface of the channels because of an overestimation of the silicalite-1/methane interaction, relative to the methane/methane one.

Note that the advantage of the *ab initio* fitted model is the one-to-one correspondence between the *ab initio* and the fitted energies. This is in contrast to the force-field model, where the parameters are adjusted to yield the experimental value, such as the diffusion coefficient. However, because the experimental data for the radial distribution function are not yet available for the investigated system, the contradiction between the structural data yielded from the *ab initio* fitted and the empirical force field remains unresolved.

To describe the behavior observed in our study (the concentration dependence of the structural properties of the methane molecule in silicalite-1 detected by the *ab initio* fitted potential), the percentages of time the molecules spend in the three resident sites (interaction, zigzag channel, and straight channel) and their ratios at various loadings are calculated and summarized in Table 1. Here, borders between the three channels were defined by the four linkage 10-oxygen-membered rings around

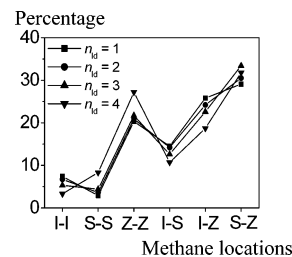


**Figure 4.** Relative residences of a pair of methane molecules at various loadings ( $n_{ld}$ ) lied under the first peak (for  $n_{ld} \leq 3$ ) and the first two peaks (for  $n_{ld} = 4$ ) of the C–C RDFs (Figure 3a); I, S, and Z respectively denoted for intersection, straight, and zigzag portions (see the text for more details).

**Table 1. Percentage of Time that the Molecules Spend in Various Resident Sites of Intersection and Zigzag and Straight Channels and Their Ratios at Various Loadings ( $n_{ld}$  = Number of Methane Molecules Per Intersection)**

$n_{ld}$	percentage			ratio		
	intersection (I)	straight channel (S)	zigzag channel (Z)	Z/S	Z/I	S/I
1	27.5	19.6	52.9	2.7	1.9	0.7
2	26.0	23.5	50.4	2.1	1.9	0.9
3	23.7	25.9	50.4	1.9	2.1	1.1
4	18.0	29.0	53.1	1.8	2.95	1.6

the intersection. Therefore, the intersection and the straight channel were separated by the two 10-oxygen-membered rings perpendicular to the  $y$  axis (see Figure 1), while the other two rings were denoted as the border between the intersection and the zigzag channel. In addition, the pair of methane molecules lying under the peaks of the C–C RDF of each concentration, counted up to the second minimum for  $n_{ld} = 4$  and to the first minimum for other concentrations (Figure 3), have been classified by their locations in 6 groups, in which both methane molecules reside in the channels of the same type,  $I_i-I_j$ ,  $S_i-S_j$ , and  $Z_i-Z_j$ , and different type,  $I_i-S_j$ ,  $I_i-Z_j$ ,  $S_i-Z_j$ , where I, S, and Z denote intersection and straight and zigzag channels, respectively, while  $i$  and  $j$  are the channels' indexes. Then, the relative frequency of occurrence of the pairs have been computed and plotted in Figure 4.

In Table 1, almost half of the methane molecules (for all concentrations) were observed to reside in the zigzag channels and about a quarter of them were distributed in the straight and intersection channels. Special interest is centered on an intensification of methane density in the straight and zigzag channels but a decrease in the intersection when the loading increases, in particular, at the  $n_{ld} = 4$ . These transformations consequently lead to a growth of the corresponding pairs of methane molecules (the C–C distances shorter than those of the second minimum in the C–C RDF shown for  $n_{ld} = 4$  in Figure 3), in which both of them locate in the  $S_i-S_j$  and  $Z_i-Z_j$  channels and a reduction of the percentage of the other pairs, in which both molecules lie in the  $I_i-I_j$  channels ( $i$  can be the same or different from  $j$ ), Figure 4. A positive contribution because of an increase in the molecular pairs locating in the same channels ( $S_i-S_j$  and  $Z_i-Z_j$ , where  $i = j$ ) leads directly to the establishment of the first peak at 5.4 Å of the C–C RDF for  $n_{ld} = 4$ , while those where  $i \neq j$  are the sources of the second sharp peaks at 7.4 Å. These conclusions have been drawn owing to the schematic representation of the related distances shown in Figure 1, in which the lengths of the straight and zigzag channels can accommodate the two methane molecules with a separation of 5.4 Å; i.e., two methane molecules can be located in  $S_i-S_j$  and  $Z_i-Z_j$ , where  $i = j$ . On the other hand,

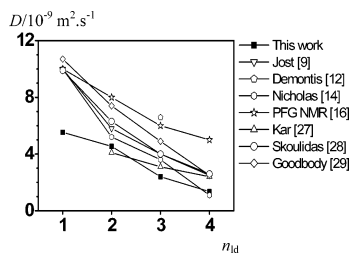


**Figure 5.** Self-diffusion coefficients ( $D$ ) at various loadings ( $n_{ld}$ ) obtained from this and various studies.

the molecular pair with the separations of 7.4 Å can be assigned to those located in  $S_i-S_j$  and  $Z_i-Z_j$ , where  $i \neq j$  (see also Figure 1).

**3.2 Self-Diffusion Coefficient.** The diffusion coefficients ( $D$ ) are calculated from different moments of the particle displacements averaged over the  $x$ ,  $y$ , and  $z$  directions.<sup>24–26</sup> The results are displayed in Figure 5 as a function of loading ( $n_{ld}$ ), in comparison with those obtained from other theoretical simulations<sup>9,12,14,27–29</sup> and PFG–NMR experiments.<sup>16</sup>

Our results are in reasonable agreement with the available data but noticeably lower in particular with respect to dilute loading ( $n_{ld} = 1$ ). This observation can be understood because of the fact that the simulated diffusion coefficient is rather sensitive to the absolute value of the depth of the potential well of the interaction energy. This is not the case for the structural data in which the shape of the potential-energy surface was generally known to play a more important role.

Discrepancy of the interaction potential can be due to a technical setback during the calculations of the *ab initio* data points in the development of the intermolecular potential function. Previous to the energy calculations, fragments were initially chosen to represent the silicalite-1 unit. The dangling bonds of the silicon atoms have to be filled up by hydrogen atoms.<sup>11,17</sup> As a consequence, each energy point mechanically incorporates a supplementary interaction owing to those hydrogen atoms. Such a problem, because of the limitations of today's computer, is generally known.<sup>30–32</sup> The only way to solve this is to increase the size of the system treated in quantum chemical calculations, which is technically impossible, especially in the development of the *ab initio* derived potential function, where numerous data points are practically required.<sup>11,17</sup> In addition, although the discrepancy in the total interaction energy is configuration-dependent, it is assumed not to affect the shape of the potential-energy surface because the same level of accuracy was applied for all data points.

**3.3 Anisotropy Effect.** To examine the anisotropic character of the system, diffusion coefficients in different directions have been investigated. The diffusional anisotropy defined as the ratio between those in  $x$  and  $y$

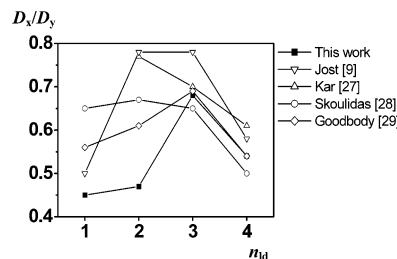


**Figure 6.** Ratio of the self-diffusivities ( $D$ ) along  $x$  and  $y$  directions in silicalite-1 at 300 K obtained from this and various studies.

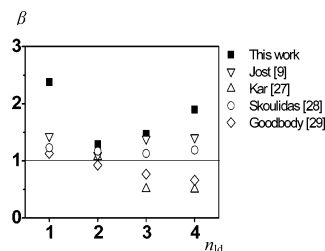


**Figure 7.**  $\beta$  obtained from eq 1 as a function of loading ( $n_{ld}$ ) obtained from this and various studies.

directions ( $D_x/D_y$ ) is given in Figure 6 in comparison with available data.<sup>9,27–29</sup>

In comparison between various force-field and our *ab initio* models, the data display a large variation at  $n_{ld} \leq 2$  and a good agreement at higher loadings. These events can be understood by the fact that, at high loadings, a substantial amount of methane molecules is restricted in a limited space inside the silicalite pores. This steric effect dominates discrepancies because of the potential functions used. On the contrary, the molecules can move and diffuse in a channel without restraint at sufficiently low loadings ( $n_{ld} \leq 2$ ). Therefore, the movements are almost controlled by the potential employed; i.e., the diffusivity depends strongly on the methane/methane and the silicalite-1/methane interactions. The large deviation at  $n_{ld} \leq 2$  indicates an artifact among the available models.

In addition to the  $D_x/D_y$  ratio, another quantity,  $\beta$ , proposed by Kärger and regularly used to characterize diffusional anisotropy in porous materials, has been examined.<sup>33</sup> The calculated  $\beta$  factors at various loadings have been calculated according to

$$\beta = \frac{c^2/D_z}{(a^2/D_x + b^2/D_y)} \quad (1)$$

where  $a$ ,  $b$ , and  $c$  are the unit-cell lengths and  $D_x$ ,  $D_y$ , and  $D_z$  are diffusion coefficients along  $x$ ,  $y$ , and  $z$  axes, respectively. The results are displayed in Figure 7.

In good agreement with the previous reports,<sup>9,27,28</sup> the  $\beta$  values for almost all models and all loadings are larger than 1.0, indicating a continuation movement along the same channel through the intersection (see Figure 1). However, the  $\beta$  values at  $n_{ld} \geq 2$  taken from refs 27 and 29 are in contrast to the other models.

**3.4 Heat of Adsorption.** The heats of adsorption ( $H$ ), which can be approximated for low density as

$$\langle H \rangle = \langle U \rangle - RT \quad (2)$$

are reported at various loadings in Figure 8, where  $\langle U \rangle$  is the silicalite-1/methane ensemble energy average. The

(24) Kärger, J.; Pfeifer, H.; Heink, W. *Principles and Applications of Self-Diffusion Measurements by Nuclear Magnetic Resonance: Advances in Magnetic Resonance*; Academic Press: New York, 1988; Vol. 12.

(25) Haberlandt, R.; Kärger, J. *Chem. Eng. J.* **1999**, *74*, 15.

(26) Fritzsche, S.; Haberlandt, R.; Kärger, J.; Pfeifer, H.; Heinzinger, K. *Chem. Phys. Lett.* **1992**, *198*, 283.

(27) Kar, S.; Chakravarty, C. *J. Phys. Chem. A* **2001**, *105*, 5785.

(28) Skoulidas, A. I.; Sholl, D. S. *J. Phys. Chem. B* **2002**, *106*, 5058.

(29) Goodbody, S. J.; Wanatabe, K.; MacGowan, D.; Walton, J. P. R. B.; Quirke, N. *J. Chem. Soc., Faraday. Trans.* **1991**, *87*, 1951.

(30) Goellner, J. F.; Gates, B. C.; Vayssilov, G. N.; Rösch, N. *J. Am. Chem. Soc.* **2002**, *122*, 8056.

(31) van Santen, R. A. *Catal. Today* **1997**, *38*, 377.

(32) Sauer, J.; Ugliengo, P.; Garrone, E.; Saunders, V. R. *Chem. Rev.* **1994**, *94*, 2095.

(33) Kärger, J. *J. Phys. Chem.* **1991**, *95*, 5558.

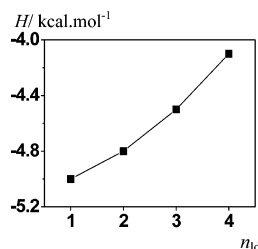


**Figure 8.** Heat of adsorption ( $H$ ) defined in eq 2 as a function of loading ( $n_d$ ).

result displays a gradual increase of  $H$  as a function of loading. In general, changes of heat of adsorption depend on two factors. A primary factor is owing to site heterogeneities. The secondary account is from the interaction between guest–guest molecules.

In regard to the percentages of methane molecules lying in each channel (Table 1) and of the pair of methane molecules classified by their locations in the two channels (Figure 4, also see the corresponding text for more details), the site heterogeneity was found to be the source of

increasing of the heat of adsorption. The conclusion was confirmed by the decrease of methane density in the intersection but an increase in the straight and zigzag channels when the concentration increases to  $n_d = 4$ . In addition, reliability of the calculated heat of adsorption at almost all loading is supported by the calorimetric values of approximately 4 kcal mol<sup>-1</sup>.<sup>34</sup>

**Acknowledgment.** This work was financially supported by the Thailand Research Fund (TRF). C. B. acknowledges a DAAD–Royal Golden Jubilee Scholarship, Grant A/99/16872, and a Royal Golden Jubilee Scholarship, Grant PHD/0090/2541. R. H. and S. F. also thank the DFG (Sonderforschungsbereich 294) for financial support. Computing facilities were provided by the Austrian–Thai Center for Chemical Education and Research at Chulalongkorn University.

LA046845W

(34) Dunne, J. A.; Mariwala, R.; Rao, M.; Sircar, S.; Gorte, R. J.; Myers, A. L. *Langmuir* **1996**, *12*, 5888.